HHS Public Access

Author manuscript

Biochemistry. Author manuscript; available in PMC 2017 August 31.

Published in final edited form as:

Biochemistry. 2017 March 14; 56(10): 1504–1517. doi:10.1021/acs.biochem.6b01221.

The Polybasic Region of the Polysialyltransferase ST8Sia-IV Binds Directly to the Neural Cell Adhesion Molecule, NCAM

Gaurang P. Bhide[†], **Gerd Prehna**[‡,§], **Benjamin E. Ramirez**[†,‡], and **Karen J. Colley**[†,*]

[†]Department of Biochemistry and Molecular Genetics, University of Illinois at Chicago, Chicago, Illinois 60607, United States

[‡]Center for Structural Biology, Research Resources Center, University of Illinois at Chicago, Chicago, Illinois 60607, United States

[§]Department of Microbiology and Immunology, University of Illinois at Chicago, Chicago, Illinois 60612, United States

Abstract

Polysialic acid (polySia) is a unique post-translational modification found on a small set of mammalian glycoproteins. Composed of long chains of α2,8-linked sialic acid, this large, negatively charged polymer attenuates protein and cell adhesion and modulates signaling mediated by its carriers and proteins that interact with these carriers. PolySia is crucial for the proper development of the nervous system and is upregulated during tissue regeneration and in highly invasive cancers. Our laboratory has previously shown that the neural cell adhesion molecule, NCAM, has an acidic surface patch in its first fibronectin type III repeat (FN1) that is critical for the polysialylation of *N*-glycans on the adjacent immunoglobulin domain (Ig5). We have also identified a polysialyltransferase (polyST) polybasic region (PBR) that may mediate substrate recognition. However, a direct interaction between the NCAM FN1 acidic patch and the polyST PBR has yet to be demonstrated. Here, we have probed this interaction using isothermal titration calorimetry and nuclear magnetic resonance (NMR) spectroscopy. We observe direct and specific binding between FN1 and the PBR peptide that is dependent upon acidic residues in FN1 and basic residues of the PBR. NMR titration experiments verified the role of the FN1 acidic patch in the recognition of the PBR and suggest a conformational change of the Ig5–FN1 linker region following binding of the PBR to the acidic patch. Finally, mutation of residues identified by NMR

[*]Corresponding Author: Department of Biochemistry and Molecular Genetics, The University of Illinois at Chicago, College of Medicine, 900 S. Ashland Ave., MC 669, Chicago, IL 60607. Phone: 312-996-7756. karenc@uic.edu.

ORCID

Karen J. Colley: 0000-0002-3801-071X

Notes

The authors declare no competing financial interest.

Supporting Information

The Supporting Information is available free of charge on the ACS Publications website at DOI: 10.1021/acs.biochem. 6b01221. Primers used for plasmid construction and mutagenesis (Supplemental Table 1), SDS–polyacrylamide gel showing purified NCAM FN1, SUMO-PBR, and their respective mutants, circular dichroism results comparing folding of NCAM FN1 and its DEE to RRR mutant, and size exclusion chromatography of FN1 and SUMO-PBR and their respective mutants (Supplemental Figure S1), HSQC spectrum of ^{15}N-labeled NCAM FN1 showing the residue assignments and prediction of secondary structure based on those assignments (Supplemental Figure S2), a replicate of HSQC NMR titration at five different FN1:SUMO-PBR ratios and saturation (Supplemental Figure S3), and localization of NCAM mutants A539S, E543R, and W545A using indirect immunofluorescence microscopy (Supplemental Figure S4) (PDF)

titration experiments impacts NCAM polysialylation, supporting their mechanistic role in protein-specific polysialylation.

Graphical Abstract

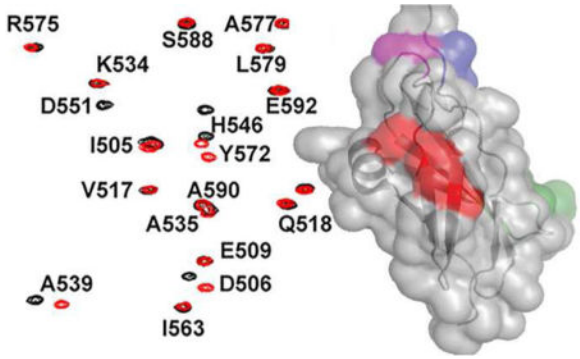

Polysialic acid (polySia) is a glycopolymer that consists of 8–400 α2,8-linked sialic acid residues that is polymerized on the glycans of a small set of mammalian glycoproteins by two Golgi-localized polysialyltransferases (polySTs), ST8Sia-II and ST8Sia-IV.[1–3] PolyST substrates include the neural cell adhesion molecule (NCAM), neuropilin-2 (NRP-2), synaptic cell adhesion molecule-1, the CD-36 scavenger receptor in human milk, the voltage-gated sodium channel α subunit, C–C chemokine receptor-7, E-selectin ligand-1, and the polySTs themselves.[4–13] This large, negatively charged polymer binds significant quantities of water and increases the hydrodynamic radius of the proteins it modifies.[14] Consequently, polySia not only abrogates cell–cell adhesion mediated by these proteins but also is believed to impact adhesion mediated by other nonpolysialylated proteins on the same cell. For example, *in vitro* studies demonstrated that polySia on NCAM is sufficient to eliminate adhesion mediated by adjacent E-cadherin molecules.[15] Furthermore, the presence of polySia has been suggested to modulate cell signaling as a reservoir for various neurotransmitters, growth factors, and chemokines and by altering *cis* (between proteins on the same membrane) and *trans* (between proteins on apposing cells) homophilic and heterophilic protein–protein interactions.[1,3] For instance, enzymatic removal of polySia alters NCAM heterophilic interactions triggering differentiation, increased survival, and reduced proliferation of neuroblastoma cells via activation of extracellular signal-regulated kinase (ERK).[16] Moreover, Eggers et al.[17] provided evidence that removing polySia promotes NCAM-dependent signaling through the Src family kinase, $p59^{Fyn}$, paxillin, and focal adhesion kinase (FAK), and this signaling increases the number of focal adhesions leading to enhanced cell–matrix interactions.

Because of the functions mentioned above, polySia has been found to be critical for nervous system development. Elimination of both polySTs in mice results in smaller overall body and brain size, a reduction in olfactory bulb size, defects in motor neuron fasciculation and axon guidance, hydrocephaly, and death within 4 weeks of birth.[18] In adults, restricted polySia expression in the hippocampus, hypothalamus, and olfactory bulb is essential for continued synaptic plasticity and cell migration.[14] Temporary re-expression of polySia has been observed following nerve and liver damage and promotes migration of precursor cells

to aid regeneration.[19,20] Strikingly, polySia is upregulated in several highly metastatic cancers, including non-small cell and small cell lung carcinoma (SCLC), neuroblastoma, Wilm's tumor, astrocytoma, colorectal carcinoma, and breast cancer.[21,22]

Our laboratory has extensively characterized the substrate specificity exhibited by polySTs. Following the early work of Nelson et al.[23] that suggested the importance of NCAM FN1 for the polysialylation of *N*-glycans in the Ig5 domain, we performed extensive polysialylation and binding studies using NCAM domain deletion mutants and showed that the first fibronectin type III repeat (FN1) of NCAM has recognition elements that recruit polySTs to polysialylate *N*-glycans in the adjacent fifth immunoglobulin domain (Ig5). We found that the Ig5–FN1 tandem is sufficient for NCAM polysialylation and that deletion of the FN1 domain from NCAM abolishes polyST–NCAM binding and NCAM polysialylation.[24–26] A crystal structure of the NCAM FN1 domain confirmed the existence of an acidic patch, formed by residues Asp^{520}, Glu^{521}, and Glu^{523} found on the surface of this domain.[27,28] Replacing these acidic residues with arginines resulted in the complete loss of NCAM polysialylation.[25] These data and more recent analysis of NRP-2 have given rise to a model in which polySTs dock to the recognition domain, and this positions them to polysialylate glycans on an adjacent domain or region. Specifically, the FN1 domain of NCAM and the meprin-A5 protein-μ tyrosine phosphatase (MAM) domain of NRP-2 are critical for polyST recognition, and this allows the polysialylation of *N*-glycans on the adjacent NCAM Ig5 domain and *O*-glycans on the adjacent NRP-2 linker region.[25,29,30] Mutating surface acidic patch residues (Asp^{520}, Glu^{521}, and Glu^{523} in NCAM and Asp^{652} and Asp^{653} in NRP-2) reduces the level of polysialylation of these proteins.[25,30] A similar two-domain paradigm is likely and has been previously suggested for the SynCAM 1 Ig2 domain (recognition) and Ig1 domain (polysialylation).[31]

Considering the polyST sequence requirements for substrate recognition, we previously identified a polybasic region (PBR) in both the polySTs, which is not found in other sialyltransferases. The polySTs are type II Golgi-localized glycosyltransferases with short N-terminal cytoplasmic tails and transmembrane regions followed by large C-terminal lumenal domains (Figure 1). This lumenal domain contains sequences conserved in all sialyltransferases called sialyl motifs [large (SML), small (SMS), motif 3 (M3), and very small (SMVS)] that bind the CMP-sialic acid donor and glycan acceptors and contain residues that are important for catalysis.[32,33] The PBR and the polysialyltransferase domain (PSTD) are unique to the polySTs and are likely involved in substrate binding and polySia chain elongation.[34–36] We found that mutation of Arg^{82} and Arg^{93} in the ST8Sia-IV PBR to alanines caused a significant reduction in the level of NCAM polysialylation.[36] Additionally, both a catalytically inactive ST8Sia-IV H331K mutant and a membrane-associated fragment derived from first 140 amino acids of this enzyme that includes the PBR were capable of serving as competitive inhibitors of NCAM polysialylation by wild-type ST8Sia-IV in transfected COS-1 cells.[34] Replacing Arg^{82} and Arg^{93} in the PBR with alanines in the inactive ST8Sia-IV H331K mutant eliminated its ability to serve as a competitive inhibitor of NCAM polysialylation, suggesting that these PBR residues are essential for NCAM recognition.[34]

While our previous studies suggest a direct interaction between the FN1 acidic patch residues and the basic residues found in the ST8Sia-IV PBR, this has yet to be shown. Demonstration of a direct interaction is needed to precisely define the mechanism of protein-specific NCAM polysialylation, as well as the interaction surface that could be targeted therapeutically. Structural characterization of polySTs and other sialyltransferases has been hindered by difficulties in obtaining recombinant enzymes in the quantity and purity that is necessary for biophysical methods (discussed in ref 37). To date, of the approximately 20 mammalian sialyltransferases, only ST3Gal-I, ST6Gal-I, and ST8Sia-III have been structurally characterized.[37–40] To circumvent this difficulty, here we use a purified NCAM FN1 domain and SUMO-tagged ST8Sia-IV PBR peptide fusion protein to probe their interaction directly *in vitro* using both isothermal titration calorimetry (ITC) and NMR spectroscopy. ITC demonstrates a direct interaction of the PBR peptide and the FN1 domain that is abrogated by mutation of the FN1 acidic residues or the PBR basic residues. NMR titration experiments map the entire interaction surface for the PBR on the FN1 domain and suggest a conformational change in the Ig5–FN1 linker region that is dependent upon PBR binding. Moreover, cellular analysis of polysialylation through site-directed mutagenesis of additional interaction residues revealed by the NMR titration experiments verified their importance for NCAM recognition by ST8Sia-IV. Finally, as we have shown that a small recombinant peptide is sufficient to target and bind a polyST substrate, our work provides the proof of principle for the use of the PBR peptide and analogues for development as a potential therapeutic.

MATERIALS AND METHODS

Reagents

The pET14(b)-6xHis-SUMO vector was a kind gift from A. Lavie (University of Illinois at Chicago). The QuikChange II Site Directed Mutagenesis Kit was from Agilent (Santa Clara, CA). PCR SuperMix High Fidelity, cell culture media Dulbecco's modified Eagle's medium (DMEM) and Opti-MEM, Lipofectamine 2000 transfection reagent, and anti-V5 mouse monoclonal antibody were purchased from Thermo-Fisher Scientific (Waltham, MA). Restriction enzymes and T4 DNA ligase were obtained from New England Biolabs (Ipswich, MA). Oligonucleotide primers were from Integrated DNA Technologies (Coralville, IA). Isopropyl β-D-1-thiogalactopyranoside (IPTG) and 2-(*N*-morpholino)ethanesulfonic acid (MES) were acquired from Gold Biotechnology (Olivette, MO). [^{13}C]Glucose and [^{15}N]ammonium chloride were obtained from Cambridge Isotope Laboratories (Tewksbury, MA). Nickel-nitrilotriacetic acid (Ni-NTA) beads were acquired from Clontech (Mountain View, CA). Molecular weight markers, 4–15% precast polyacrylamide gels, and Clarity Western ECL Substrate were purchased from Bio-Rad (Hercules, CA). Nitrocellulose membranes and protein A-Sepharose beads were from GE Healthcare (Little Chalfont, U.K.). HyBlot CL autoradiography films were from Denville Scientific Inc. (Denville, NJ). The anti-polySia 12F8 and anti-6xHis antibodies were purchased from BD Biosciences (San Jose, CA). Horseradish peroxidase (HRP)- and fluorescein isothiocyanate (FITC)-conjugated secondary antibodies were obtained from Jackson ImmunoResearch (West Grove, PA). All other reagents were purchased from Sigma-Aldrich, Fisher Scientific, or VWR International (Radnor, PA).

Construction of the 6xHis-SUMO-PBR Bacterial Expression Construct

ST8Sia-IV residues 75–100 were amplified with the NdeI restriction site at the N-terminus and the BamHI restriction site at the C-terminus using primers 5′-CATATGTCCTCTTTGGTCCTAGAG-3′ and 5′-AAGAATCGCAGGTTTAAGTAGGGATCCGGCT-3′, respectively. Amplified ST8Sia-IV sequences and the vector mentioned above were digested with NdeI and BamHI restriction endonucleases and purified on an agarose gel. The insert was then ligated into the vector using T4 DNA ligase generating the 6xHis-SUMO-PBR plasmid.

Mutagenesis of 6xHis-FN1, 6xHis-SUMO-PBR, and Full-Length NCAM

Mutagenesis was performed in all the constructs mentioned above using the primer sets listed in Supplemental Table 1 and the QuikChange II site-directed mutagenesis kit according to the manufacturer's protocol. Isolated clones were sequenced by Sanger sequencing at the DNA Services Facility of the University of Illinois at Chicago Research Resources Center and were checked for accuracy using SnapGene Viewer software (GSL Biotech).

Expression and Purification of the 6xHis-FN1, 6xHis-SUMO, and 6xHis-SUMO-PBR Proteins

6xHis-FN1 was purified as previously described.[27] Briefly, BL21(DE3) CodonPlus *Escherichia coli* cells expressing 6xHis-FN1 were grown in 2xYT medium at 37 °C. The culture was then induced with 1 mM IPTG at an optical density (λ = 600 nm) of 0.6–0.8 and maintained overnight at 22 °C. For isotopically labeled 6xHis-FN1, cells were grown in M9 minimal medium containing 1 g of [^{15}N]ammonium chloride and/or 5 g of [^{13}C]glucose per liter. The cells were harvested by centrifugation and lysed using Avestin Emulsiflex C5. The cleared supernatant was passed over the Ni-NTA column to bind the His-tagged protein. The column was washed with a buffer consisting of 50 mM Tris-HCl (pH 8.0), 500 mM NaCl, and 50 mM imidazole. The protein was eluted in the same buffer containing 500 mM imidazole. The protein was then dialyzed in the same buffer without the imidazole overnight at 4 °C for the ITC experiments and in a buffer containing 300 mM NaCl and 20 mM KH_2PO_4 (pH 6.6) for the NMR experiments. To obtain 6xHis-SUMO and 6xHis-SUMO-PBR, BL21(DE3) C41 *E. coli* cells expressing this construct were grown in 2xYT medium at 37 °C to an optical density (λ = 600 nm) of 0.8–1.0 and induced with 1 mM IPTG. The growth was continued at 37 °C for 4 h, and cells were harvested thereafter. The 6xHis-SUMO-PBR peptide was purified as described above.

Isothermal Titration Calorimetry

Purified 6xHis-FN1, its (DEE → RRR) mutant, 6xHis-SUMO, 6xHis-SUMO-PBR, and its (R82A/R93A) mutant were dialyzed overnight at 4 °C in a buffer containing 500 mM NaCl and 50 mM Tris (pH 8). FN1 and its mutant were prepared at a concentration of 20 μM, and the PBR peptide and its mutant were concentrated to 600 μM. All the experiments were performed at 25 °C using a VP-ITC calorimeter (GE Healthcare). The final thermodynamic parameters were calculated using Origin software (GE Healthcare) using a one-site model.

NMR Spectroscopy

$^{1}H–^{15}N$ HSQC, HNCA, HNCO, HN(CA)CO, HN(CO)CA, HNCACB, and CBCACONH spectra for FN1 backbone assignments were recorded at 25 °C on a Bruker 600 MHz DRX spectrometer equipped with a 5 mm inverse cryogenic probe. NMR spectra for HSQC titrations were recorded on a Bruker 900 MHz AVANCE spectrometer equipped with a 5 mm TCI cryogenic probe. Samples for all the NMR experiments were in a buffer containing 300 mM NaCl and 20 mM KH_2PO_4 (pH 6.6), supplemented with 10% D_2O. Backbone dihedral angles and the secondary structure of FN1 were predicted using Talos+.[41] All NMR data were processed using NMRPipe[42] and analyzed using UCSF Sparky. HSQC titrations were recorded in a 5 mm NMR tube at 1:0 (8 scans), 1:5 (32 scans), and 1:10 (64 scans) ratios of FN1 to 6xHis-SUMO-PBR and its mutant (R82A/R93A).

Circular Dichroism Spectroscopy

Purified FN1 was prepared at a concentration of 75 μg/mL in 300 mM NaF and 20 mM $KHPO_4$ (pH 6.5), and its CD spectrum was recorded in a 0.1 cm path-length cuvette on a Jasco-815 spectropolarimeter from a wavelength of 190–260 nm. The ellipticity per residue in degrees square centimeter per decimole was plotted against the wavelength to compare the secondary structures of FN1 to that of its DEE to RRR mutant.

Gel Filtration

The 6xHis-SUMO-PBR and 6xHis-SUM-OPBR (R82A/R93A) mutant were purified and concentrated at 5 mg/mL in a buffer containing 20 mM Tris-HCl (pH 8) and 500 mM NaCl and injected into an AKTA protein purification system (GE Healthcare) connected to a Superdex 75 10/300 GL size exclusion chromatography column (GE Healthcare).

Transfection of COS-7 Cells for Immunoprecipitation and Immunoblotting

COS-7 cells were maintained in DMEM supplemented with 10% FBS and 1% penicillin-streptomycin in a 37 °C, 5% CO_2 incubator. Cells plated in 100 mm tissue culture plates were transfected at 80–90% confluence the next day with 5 μg each of V5-tagged NCAM and ST8Sia-IV cDNAs in 3 mL of Opti-MEM medium using 20 μL of Lipofectamine 2000 per plate, according to the manufacturer's protocol. The cDNAs described above were made as described previously.[26,36] Shortly after the addition of the DNA complexes to the cells, 7 mL of DMEM supplemented with 10% FBS was added to the cells and cells were incubated for 24 h at 37 °C and 5% CO_2.

Immunoprecipitation of V5-Tagged NCAM and Its Mutants

Twenty-four hours post-transfection, cells were lysed and immunoprecipitation was performed using an anti-V5 antibody and protein A-Sepharose beads, as described previously.[30]

Immunoblot Analysis of NCAM and Mutant Protein Polysialylation

Immunoprecipitated V5-tagged NCAM and NCAM mutants were heated at 65 °C for 8 min with Laemmli sample buffer [62.5 mM Tris-HCl (pH 6.8), 25% glycerol, 2% SDS, and 0.01% bromophenol blue] containing 10% β-mercaptoethanol to preserve polySia. To

analyze expression of NCAM and its mutants, a 10% aliquot of the cleared cell lysate was boiled with Laemmli sample buffer for 8 min. Proteins were then separated by electrophoresis on a 4 to 15% precast polyacrylamide gel and transferred onto nitrocellulose membranes for 1 h at 100 V. The membranes were blocked for 1 h in 5% nonfat dry milk in TBST {Tris-buffered saline [TBS, 50 mM Tris-HCl (pH 8.0) and 150 mM NaCl] and 0.1% Tween 20} and incubated overnight at 4 °C in a 1:1500 dilution of the 12F8 anti-polySia monoclonal antibody in 2% milk in TBS to analyze polysialylation or a 1:10000 dilution of the anti-V5 monoclonal antibody in 5% nonfat dry milk in TBST to analyze the expression of NCAM mutants. After being washed four times for 10 min each with TBST with agitation, the membranes were incubated with a 1:5000 dilution of HRPconjugated goat anti-rat IgM (12F8) and goat anti-mouse IgG (anti-V5) secondary antibodies in 5% blocking buffer in TBST for 1 h. After being washed four times for 10 min each in TBST with agitation, the membranes were developed using Clarity Western ECL Substrate and HyBlot CL autoradiography film. To compare polysialylation levels of different NCAM mutants, we used ImageJ (National Institutes of Health) for densitometry and calculated the ratio of polysialylated protein level to loading control protein level for each mutant with the value for wild-type NCAM set to 100%. The mean and standard deviation (SD) were calculated. Statistical analysis was performed using unpaired Student's t tests to provide the p values shown in the figures.

Cellular Localization of NCAM Mutants

COS-7 cells plated on 12 mm glass coverslips in 24-well plates were transfected at 80–90% confluence with 500 ng of V5-tagged NCAM or NCAM mutant protein expression vectors mixed with 1 μL of Lipofectamine 2000 and 150 μL of Opti-MEM I medium per well. One milliliter of DMEM containing 10% FBS was added to each well and incubated for 24 h. Thereafter, cells were washed twice with PBS and fixed and permeablized in −20 °C methanol. Detection of proteins by indirect immunofluorescence microscopy was performed as described previously.[30] Briefly, fixed and permeabilized cells were incubated with mouse monoclonal anti-V5 antibody (Thermo-Fisher) in blocking buffer (5% normal goat serum in PBS) and stained with FITC-conjugated goat anti-mouse IgG and 4′,6-diamidino-2-phenylindol (DAPI) to stain the nucleus. Cells were visualized and imaged using a Zeiss LSM 700 inverted confocal microscope equipped with an AxioCam digital microscope camera using a 100× oil-immersion lens. Images were acquired using Zen software (Zeiss) and analyzed using ImageJ (National Institutes of Health).

RESULTS

The Recombinant ST8Sia-IV PBR Peptide and the NCAM FN1 Acidic Patch Interact Directly *in Vitro*

Given the difficulty in obtaining full-length recombinant ST8Sia-lV, we sought to focus solely on the PBR of the protein. Initial biochemical experiments attempted to use a chemically synthesized PBR peptide consisting of residues 71–105 (Figure 1A); however, the peptide was largely insoluble in physiological buffers likely because of its high hydrophobicity. To circumvent this technical problem, we engineered a bacterial expression vector consisting of an N-terminal 6xHis-SUMO tag linked to the ST8Sia-IV PBR peptide

(residues 75–100) (henceforth termed SUMO-PBR) (Figure 1A). The length of this peptide was chosen to include residues critical for recognition and polysialylation of NCAM[34,36] while excluding surrounding hydrophobic residues to improve solubility. According to the models of full-length ST8Sia-IV and the PBR published by Volkers et al.[38] and Zhou et al.,[43] the peptide should include the entire helical region on the N-terminal end of the PBR and a smaller helix at the C-terminus connected by a loop. Moreover, the two basic residues not included in our peptide, Lys^{72} and Lys^{103}, have little to no effect on NCAM polysialylation when they are mutated to alanines, as previously reported by our laboratory.[36] The addition of a protein affinity tag permitted purification from *E. coli* lysates and aided in maintaining solubility. The FN1 domain was expressed and purified as described previously (Figure S1).[27]

As we could obtain pure recombinant protein, we chose ITC to assay for a direct interaction and to probe in detail the residues involved in binding. Concentrated SUMO-PBR peptide was titrated into dilute FN1 at a ratio of 30:1, revealing a direct interaction *in vitro* (Figure 1B). After the background heats had been subtracted from the SUMO control, the molecular interaction between the ST8Sia-IV PBR and the NCAM FN1 domain exhibited a 1:1 (N = 1.060 ± 0.0698) stoichiometry and a K_d of 10 μM (10.88 ± 2.46 μM) using a one-site binding model. This model was chosen on the basis of our past work[24] and recent modeling studies showing a 1:1 ST8Sia-IV:Ig5–FN1 stoichiometry.[38] The interaction exhibited an enthalpic contribution (ΔH of approximately −1 kcal/mol or 990.6 ± 91 cal/mol) and was also entropically favorable (ΔS of 19.39 cal K^{-1} mol^{-1}), implying that the hydrophobic nature of the PBR also contributes to the recognition of NCAM FN1.[44] However, this could also be reflective of the induction of local disorder in another part of FN1. A change in protein dynamics upon ligand binding to offset potential entropic penalties can be observed, as noted in the work of MacRaild et al.[45]

To further assess whether this binding event requires specific electrostatic interactions as previous research has suggested,[25,36] we purified both PBR and FN1 domain mutants and assayed binding by ITC (Figure 1C,D and Figure S1). Replacing Asp^{520}, Glu^{521}, and Glu^{523} of FN1 [D520, E521, and E523 with three arginines (DEE to RRR)] in full-length NCAM results in abrogation of polysialylation.[25] This FN1 mutant no longer binds to NCAM as observed with ITC (Figure 1C). Similarly, mutation of the key basic residues (Arg^{82} and Arg^{93}) in the PBR peptide [SUMO-PBR (R82A/R93A)] resulted in a lack of binding between the SUMO-PBR and the FN1 domain[36] (Figure 1D). Furthermore, circular dichroism and size exclusion chromatography demonstrated that FN1 (DEE to RRR) and the PBR peptide R82A/R93A mutants adopt folds similar to that of the wild-type protein, indicating that the loss of binding was not simply caused by protein misfolding or aggregation (Figure S1). Taken together, these results show for the first time that the interaction between the ST8Sia-IV PBR and the FN1 domain of NCAM is a direct binding event that depends on electrostatic interactions between specific residues.

$^{1}H–^{15}N$ HSQC Titration Experiments Reveal the FN1–ST8Sia-IV PBR Interaction Surface

As the X-ray crystal structure of the FN1 domain of NCAM is known[27] and we have shown a direct interaction with the ST8Sia-IV PBR, we sought to map the residues of the PBR

binding interface on the FN1 domain surface. To do this, we first obtained chemical shift assignments for the NCAM FN1 domain using standard heteronuclear NMR experiments with isotopically labeled protein (Figure S2, 99% complete, BMRB entry 26929). Next, the FN1 domain was titrated with purified SUMO-PBR, and $^{1}H–^{15}N$ HSQC spectra recorded (Figure 2A and Figure S3). As a control, the same titrations were performed with the SUMO-PBR (R82A/R93A) mutant that does not interact with the FN1 domain, as shown above by ITC (Figure 2B). The SUMO-PBR and FN1 titration experiments exhibited dose-dependent chemical shift perturbations for several residues, and appear to be in fast exchange as only one resonance is observed for the affected residues at each titration point (Figure 2A and Figure S3). In contrast, the SUMO-PBR (R82A/R93A) mutant showed minimal differences. This supports our ITC data and highlights those residues that are likely to interact with the PBR peptide. Regions of interest showing chemical shift perturbations relative to the control are boxed in panels A and B of Figure 2, and chemical shift perturbations are shown in more detail in Figure 2C for Thr^{499} (box 1), Glu^{521} (box 2), and Asp^{506} (box 3). Additionally, the combined shift difference was calculated as $[(\text{proton shifts})^2 + (\text{nitrogen shifts}/6.51)^2]^{0.546}$ for the FN1:SUMO-PBR and FN1:SUMO-PBR (R82A/R93A) 1:10 titration ratios. After the minimal changes had been subtracted from the control, several residues exhibiting significant chemical shift perturbations are observed (Figure 3A). These residues were then mapped to the crystal structure of the FN1 domain [Protein Data Bank (PDB) 2HAZ] and color-coded by surface and function (Figure 3B).

Included among the FN1 residues that have a significant chemical shift perturbation upon PBR peptide binding are several acidic residues, including the previously identified acidic patch residues Asp^{520} (D520) and Glu^{521} (E521) (Figure 3A,B, red). Glu^{523} is also implicated as part of the patch by both experimental evidence (ref 25 and see below) and calculated surface electrostatics (Figure 3C). However, because of a residue overlap in the $^{1}H–^{15}N$ HSQC spectrum, we could not definitively conclude that Glu^{523} displays a chemical shift difference. Additionally, the NMR spectra show a significant perturbation of Asp^{506} (D506) and Asp^{498} (D498) upon interaction with the PBR peptide (Figure 3A,B). While Asp^{506} is adjacent to the previously described acidic patch on the FN1 surface, Asp^{498} is found in the linker region between Ig5 and FN1 (Figure 3B). Nevertheless, both residues could belong to an extended acidic patch based on a map of this domain's electrostatic surface potential generated by the Adaptive Poisson–Boltzmann Solver (APBS) server[47] (Figure 3C).

As mentioned above, Asp^{498} is found in a linker region between Ig5 and FN1 (Figure 4A). This residue and the adjacent Thr^{499} display significant chemical shift perturbations upon binding of the ST8Sia-IV PBR peptide (dark blue strand, asterisks), while the adjacent linker residues, Gln^{496} and Ala^{497}, display smaller perturbations (Figure 3A, dark blue, and Figure 4A, dark blue). The Ig5–FN1 linker region is flanked by two loops, ^{526}GGVPI^{530} and ^{580}NGKG^{583}, that are essential for NCAM polysialylation; replacing the residues in these loops with alanines or glycines eliminates polysialylation (Figure 4, magenta strands).[24] The previously determined X-ray crystal structure of the NCAM Ig5–FN1 linker region indicates that the main chain amide of Asp^{498} forms a hydrogen bond with the main chain carbonyl of Gly^{526}, a member of the ^{525}GGVPI^{529} loop (Figure 4B), and the main chain carbonyl of Asp^{498} forms a hydrogen bond with the side chain carboxyl group of

Asn^{580}, part of the NGKG loop (Figure 4C).[28] These interactions have been suggested to stabilize the Ig5–FN1 linker region.[24] Strikingly, Gly^{526} and, to a lesser extent, Gly^{527} of the GGVPI loop also display a chemical shift upon PBR peptide binding (Figure 3, magenta), suggesting that either the PBR peptide contacts this region directly or the interaction of the PBR with the acidic patch or linker translates into changes in the conformation of this loop.

The NMR titration experiments also revealed a potential PBR interaction surface on the FN1 domain not previously implicated by structural studies and mutagenesis experiments. Residues Trp^{537}–Ser^{547} located in a large loop between strands β3 and β4 showed significant chemical shift perturbations (Figure S2B and Figure 3A,B, green). As this loop is found on a face of the FN1 domain opposite that of the acidic patch, it is possible that the PBR peptide used in our study binds in an extended conformation, allowing it to wrap around the surface of the FN1 to contact this region. However, this extended conformation seems to be incompatible with a hypothetical structure of the ST8Sia-IV modeled after the X-ray structure of a related α2,8-sialyltransferase, ST8Sia-III.[38]

Relative Contributions of Identified FN1 Acidic Surface Residues to NCAM Polysialylation

Having mapped the residues of the acidic patch using NMR titration experiments, we proceeded to assess their relative contribution to NCAM polysialylation by ST8Sia-IV. We have previously demonstrated that replacing residues Asp^{520}, Glu^{521}, and Glu^{523} simultaneously with alanine residues reduces the level of NCAM polysialylation, and replacing them simultaneously with arginine residues abolishes NCAM polysialylation.[25] Considering that our NMR data also suggest that Asp^{498} and Asp^{506} may be part of the acidic patch (Figure 3), we also probed their impact on NCAM polysialylation. We mutated each acidic residue individually to arginine, co-expressed the mutant NCAM proteins with ST8Sia-IV in COS-7 cells, and evaluated their polysialylation by immunoprecipitating the NCAM proteins and immunoblotting with an anti-polySia antibody (Figure 5A, top panel). In addition, the relative expression level of each protein was determined by removing an aliquot of the cell lysate prior to immunoprecipitation and evaluating protein expression by immunoblotting with an anti-V5 epitope tag antibody after boiling the sample to remove polySia (Figure 5A, bottom panel).

Replacing Asp^{498} (D498R) had the maximal impact, effectively eliminating NCAM polysialylation [4 ± 5% (SD) relative to NCAM (Figure 5A, right)]. Mutating the other acidic residues to arginine, including Asp^{506} (D506R), also produced a reduction in the level of polysialylation [61 ± 9% (SD) of wild-type levels (Figure 5A, right)]. Within the previously identified acidic patch (Asp^{520}, Glu^{521}, and Glu^{523}), individually replacing Glu^{521} and Glu^{523} with arginine (E521R and E523R, respectively) had the greatest impact on NCAM polysialylation [19 ± 6% (SD) and 12 ± 7% (SD) of wild-type levels, respectively (Figure 5A, right)]. It has been shown by our lab that this loss of polysialylation is not due to misfolding and ER mislocalization of the D520R, E521R, and E523R NCAM mutants.[25] Likewise, we found that the D498R and D506R NCAM mutants are localized at the cell surface and in the Golgi in transit to the surface, like wild-type NCAM (Figure 5C).

The decreases in the level of polysialylation of the mutant proteins suggest that a reduced level of polyST–NCAM binding in the absence of these acidic residues may impair chain

elongation, or alternatively, their absence may compromise polyST docking and alter access to one of the two *N*-glycan sites that are polysialylated in wild-type NCAM. However, we must consider that Asp^{498} chemical shift perturbations upon PBR peptide binding and the elimination of polysialylation in the D498R mutant could reflect a change in conformation in the Ig5–FN1 linker region after binding of the PBR peptide to the core acidic patch in FN1, as well as a requirement for specific residues in the linker region for maintenance of flexibility and/or positioning of Ig5 and FN1. Indeed, our NMR titration experiments suggest that other nonacidic residues in the Ig5–FN1 linker region are affected by the binding of the PBR (Figure 3A, dark blue, and see below).

The Ig5–FN1 Linker Region Is Important for NCAM Polysialylation

Immediately following a 6xHis tag and thrombin cleavage site (21 residues) at the very N-terminus of recombinant FN1, we included four residues of the Ig5–FN1 linker (Gln^{496}, Ala^{497}, Asp^{498}, and Thr^{499}), and all four exhibited chemical shift perturbations upon binding of the PBR peptide (Figure 3A, dark blue). Here we did a side-by-side comparison of ST8Sia-IV polysialylation of NCAM D498R and T499A mutants in COS-7 cells (Figure 5B). As discussed above, the D498R mutation resulted in a nearly complete loss of NCAM polysialylation. The T499A mutation resulted in the loss of approximately 50% of the polysialylation observed for wild-type NCAM [39 ± 24% (SD) of wild-type levels (Figure 5B)]. This decrease in the level of polysialylation was not due to misfolding and mislocalization as indirect immunofluorescence microscopy demonstrated that the T499A mutant was properly localized and observed on the cell surface and in the Golgi in transit to the surface (Figure 5C). Notably, replacing Asp^{498} with alanine (D498A) led to a decrease in the level of NCAM polysialylation to 60 ± 10% (SD) of that of the wild-type protein (M. Thompson, unpublished data).

Role of the FN1 β3–β4 Loop in the Polysialylation of NCAM

In addition to the acidic patch and residues in the Ig5–FN1 linker region, the NMR titration experiments also showed chemical shift perturbations for residues in the loop between the β3 and β4 strands of the FN1 domain (residues Trp^{537}–Ser^{547}) (Figure 3A,B and Figure 4, green). As these residues have not been previously implicated in NCAM polysialylation, we mutated them and assessed the impact on NCAM polysialylation by ST8Sia-IV in COS-7 cells (Figure 6A). We constructed five point mutations in this loop; however, only residues Ala^{539} and Trp^{545} showed changes in polysialylation, and these changes were dependent upon the amino acid substitution. For example, when Trp^{545} is mutated to alanine (W545A), this impacts polysialylation [33 ± 13% (SD) of wild-type levels] without causing the protein to misfold and mislocalize (Figure 6 and Figure S3). However, when this residue is mutated to tyrosine (W545Y), it has no substantial effect on NCAM polysialylation [91 ± 18% (SD) of wild-type levels] (Figure 6). The same pattern holds true for Ala^{539}. Mutation to serine reduces the level of polysialylation [41 ± 9% (SD) of wild-type levels], but substitution with a large aromatic residue (A539F) had a weaker effect [77 ± 5% (SD) of wildtype levels (Figure 6)].

As some of these residues in the β3–β4 loop, including Ala^{539} and Trp^{545}, appear to be conserved in fibronectin type III repeats as illustrated in the comparison of NCAM FN1 and

FN2 sequences, they likely serve to stabilize the conformation of this loop region in the protein fold (Figure 6C, purple boxes). This is apparent upon analysis of the FN1 domain crystal structure as these residues are involved in packing interactions in this region (Figure 6B). For example, the aliphatic chain of Arg^{538} packs against the aromatic ring of Trp^{545}. Similarly, Tyr^{572}, which also shows some chemical shift perturbation (Figure 3A), may be packing against Ala^{539}, and this packing would be enhanced were Ala^{539} to be replaced by phenylalanine (A539F). As for why this region may affect polysialylation, it is important to note that strands β3 and β4 along with this loop connect the acidic patch to the FN1 α-helix that has previously been shown to be important for the proper positioning of the polySTs on the surface of NCAM.[27]

Taken together, our data support the notion that as the ST8Sia-IV PBR peptide binds the NCAM FN1 core acidic patch, conformational changes are translated to the Ig5–FN1 linker region through the adjacent stabilizing GGVPI loop and to residues in the β3–β4 loop that links to both the GGVPI and the acidic patch, and that these conformational changes likely influence the Ig5–FN1 relationship, polyST positioning, and NCAM polysialylation.

DISCUSSION

In this study, we have provided biophysical evidence showing that the acidic patch of the NCAM FN1 domain is recognized directly by the PBR of ST8Sia-IV. Moreover, we have mapped the full interaction surface of the PBR on the surface of FN1 using NMR titration experiments and have shown that the chemical environments of not only the acidic patch residues but also residues in the Ig5–FN1 linker region and one adjacent loop (GGVPI) are altered upon binding of the PBR to the NCAM FN1 domain. We also observed that a distal loop region between FN1 strands β3 and β4 is affected by the binding of the PBR to FN1. This loop links to the GGVPI loop and acidic patch (Figure 4). Our data suggest that the binding of the ST8Sia-IV PBR to the NCAM FN1 acidic patch relays substantial conformational changes in the FN1 domain and linker region that likely influence its relationship to the adjacent Ig5 domain and the polysialylation of *N*-glycans in this domain. These data are discussed below in the context of other mutagenesis and binding data to provide a model of NCAM protein-specific polysialylation.

The ITC data in this work and previous mutagenesis and binding studies provide ample evidence that the NCAM FN1 domain, and particularly an acidic surface patch, are the key recognition element and a docking site for ST8Sia-IV.[25,29] Here we provide the first direct evidence that the FN1 acidic patch mediates ST8Sia-IV binding by demonstrating that replacing FN1 acidic patch residues Asp^{520}, Glu^{521}, and Glu^{523} with arginines eliminates ST8Sia-IV PBR binding. Interestingly, replacing these acidic residues with either alanines or arginines in full-length NCAM reduced the level of ST8Sia-IV binding by only ~35%,[29] suggesting that other interactions might be occurring between the full-length proteins. One possibility is that Ig5–FN1 linker residues, and especially the acidic Asp^{498}, might mediate additional contacts with the full-length enzyme. While we cannot rule out this possibility, analyses of NCAM chimeras and mutants highlighted the importance of the composition and length of the Ig5–FN1 linker region and secondary interactions between the polyST docked on the FN1 acidic patch and the Ig5 domain.[29,48]

Nevertheless, our NMR data are consistent with a role for the Ig5–FN1 linker and adjacent FN1 loop sequences in NCAM polysialylation. The chemical shift perturbations observed following binding of the PBR to the FN1 domain for Gln^{496}, Ala^{497}, Asp^{498}, and Thr^{499} of the Ig5–FN1 linker region and Gly^{526} and Gly^{527} of the GGVPI loop suggest two possibilities. First, as the core acidic patch residues are linked to the GGVPI loop by only a few amino acids, and the main chain carbonyl of Gly^{526} forms a hydrogen bond with the main chain amino group of Asp^{498} in the linker, one could envision that the binding of the ST8Sia-IV PBR to the core acidic patch may translate a conformational change to the GGVPI loop that in turn impacts the conformation of the linker. Alternatively, the acidic patch and GGVPI could be part of the binding site for the PBR. This latter possibility seems unlikely in that previous mutagenesis studies have demonstrated that neither the GGVPI or NGKG loops have a role in ST8Sia-IV binding.[24] On the other hand, replacing the proline residues in the Pro^{500}-Ser^{501}-Ser^{502}-Pro^{503} sequence (see Figure 4) on a stretch directly linked to the Gln^{496}-Ala^{497}-Asp^{498}-Thr^{499} linker not only eliminates polysialylation but also decreases the level of ST8Sia-IV binding.[24] Because ^{1}H–^{15}N HSQC NMR titrations cannot show perturbations in proline residues, we are unable to detect any changes in their chemical environment upon PBR binding. These results and other work described below suggest that the linker region, its conformation, and a defined Ig5–FN1 domain orientation are essential for NCAM polysialylation.

The importance of the Ig5–FN1 linker region orientation in polyST recognition and polysialylation was first suggested by Foley et al.,[48] who showed that inserting three amino acids between the Ig5 and FN1 domain eliminated all polysialylation of Ig5 *N*-glycans. Subsequent evaluation of mutants and chimeric proteins strongly suggested that after binding the FN1 domain, the polySTs make a necessary contact with the Ig5 domain to allow *N*-glycan polysialylation. Early experiments by Foley et al.[28] showed that insertion of new glycosylation sites into the Ig5 domain blocked the polysialylation of the original *N*-glycans and shifted polysialylation to *O*-glycans in the FN1 domain. However, experiments with chimeric proteins provided the most direct evidence of the importance of the polyST–Ig5 interaction. Thompson et al.[29] found that while the olfactory cell adhesion molecule (OCAM) itself is not polysialylated despite sharing the same domain structure and glycosylation sites as NCAM, an NCAM–OCAM chimera in which the FN1 domain of NCAM was replaced with that of OCAM is polysialylated. The OCAM FN1 domain could be recognized by ST8Sia-IV, but large basic residues in the OCAM Ig5 domain blocked polyST access and *N*-glycan polysialylation, suggesting that the polySTs make contact with amino acid sequences in this NCAM domain that are required for their proper positioning.[29] Consequently, changes in the Ig5–FN1 linker or the GGVPI or NGKG loop regions that stabilize the linker or even sequences adjacent to the linker, like PSSP, may alter the Ig5–FN1 domain orientation and block this secondary binding interaction in the Ig5 domain.

If a defined Ig5–FN1 domain orientation is essential, how can we explain the possible conformational changes we observe in the GGVPI loop and Gln^{496}-Ala^{497}-Asp^{498}-Thr^{499} linker? To evaluate the flexibility of N-glycosylation site positioning and effectively the flexibility in the Ig5–FN1 relationship, Foley et al.[28] moved consensus glycosylation sites into different positions on Ig5 and evaluated their polysialylation. The results suggested some flexibility in glycosylation site preference, particularly if the site was placed on the

same face of the Ig5 domain as one of the two glycosylation sites carrying the *N*-glycans that are typically polysialylated. We proposed a limited flexibility of the linker, constrained from side-to-side movement by the GGVPI and NGKG loops but able to move in such a way that the Ig5 domain could come closer or move farther away from the FN1 domain.[24,28] With this in mind, it is tempting to speculate that changes in the chemical environment of the GGVPI and Gln^{496}-Ala^{497}-Asp^{498}-Thr^{499} linker residues upon binding of the PBR to the acidic patch may reflect a more active Ig5–FN1 repositioning that allows a secondary interaction of the docked polyST with Ig5 sequences. Interestingly, this type of restricted flexibility in the analogous Ig5–FN1 linker of OCAM is suggested by two X-ray crystal structures of this protein.[49]

Perturbations in the $\beta3$–$\beta4$ loop region were not expected upon titration of FN1 with the PBR. However, replacing certain selected residues within this stretch affected NCAM polysialylation depending on the choice of amino acids. Some of these residues are conserved between FN1 and FN2 domains; notably, Trp^{545} is conserved among many of the fibronectin type III domains (Figure 6C). This suggests the possibility that this loop might be important for positioning various structural elements of the FN1 domain. Indeed, the $\beta3$ strand directly follows a stretch containing the acidic patch and GGVPI loop, while the $\beta4$ strand links to an α-helix consisting of residues Asp^{551}–Gly^{559} (Figure 4A). This α-helix is unique to the NCAM FN1 domain and, when replaced with two threonine or two alanine residues in full-length NCAM, does not reduce the level of NCAM polysialylation but shifts polySia from Ig5 *N*-glycans to FN1 *O*-glycans, implying that it could be important for the positioning of polySTs on the FN1 domain.[27] Notably, no chemical shift perturbations were observed for the residues in the FN1 α-helix. As a result, the chemical perturbations observed in the $\beta3$–$\beta4$ loop might be due a relayed distal conformational change or induction of local disorder as the PBR binds to the acidic patch. Additionally, although our past results show that the Ig5–FN1 linker region may dimerize,[28] the FN1 domain alone is a monomer,[27] in agreement with our SEC data (Figure S1). This strongly suggests the observed $\beta3$–$\beta4$ loop chemical exchange is not a weak dimer effect. Furthermore, we cannot rule out the possibility that this loop is an alternative binding site or involved in nonspecific interactions with the SUMO tag. However, our attempts to fit the ITC data to a two-binding site model to account for alternative and/or dual binding sites generated errors that were significantly larger than those generated when we fit the ITC data to a one-site model, supporting our interpretation of the interaction between PBR and FN1.

Recently, Volkers et al.[38] have modeled ST8Sia-IV on an X-ray crystal structure of a related $\alpha2$,8-sialyltransferase, ST8Sia-III. In this work, they docked the NCAM Ig5–FN1 structure previously determined by our laboratory[28] on the modeled ST8Sia-IV structure. In this model, Glu^{521} of the FN1 acidic patch interacts with Arg^{93} in the PBR while Glu^{523} is shown to interact with basic residues in the ST8Sia-IV polysialyltransferase domain (PSTD) (see Figure 1A). The PSTD is a stretch of 32 amino acids, rich in basic residues, found in the catalytic domain and adjacent to a conserved region in all sialyltransferases called the small sialyl motif (SMS)[35] (see Figure 1A). Mutation of select residues in the ST8Sia-IV PSTD eliminated its ability to polysialylate NCAM or autopolysialylate itself.[35,36] Nakata et al.[35] originally proposed that this region may play a role in stabilizing the growing polySia chain during the polymerization process. The model of Volkers et al.[38] suggests that this indeed

may be the case, and that the PSTD and PBR together form an extended basic groove for substrate recognition as well as processive synthesis of the growing polySia chain. Our mutagenesis data demonstrate that replacing Glu^{523} substantially decreases the level of NCAM polysialylation as detected by the anti-polySia antibody upon immunoblotting, and that the polysialylated NCAM protein detected appears to migrate at a lower molecular mass, suggesting fewer or shorter polySia chains are present (Figure 5A). Given this model, it is a plausible alternative that Glu^{523} does not interact with the PBR, even though it is adjacent to other acidic residues on the FN1 surface that do, and instead interacts with PSTD residues. Disruption of the PBR–PSTD interaction in the Glu^{523} mutant could destabilize this interaction and the basic surface for substrate recognition and/or polySia elongation.

The limited expression of polySia in adult tissues, together with its expression in many forms of cancer and its correlation with an increased level of metastasis, makes it an attractive therapeutic target. Recently, Paulson and colleagues demonstrated the global inhibition of sialylation in cells and mice using a sialic acid analogue, 3F-NeuAc.[50,51] However, the specific blockade of polysialylation has been more elusive with various treatments leading to global inhibition of sialylation and/or unexpected consequences. Seidenfaden et al.[52] demonstrated that inducing differentiation of the neuroblastoma line, SH-SY5Y, using retinoic acid simultaneously decreased the level of ST8Sia-II mRNA and dramatically increased the level of ST8Sia-IV mRNA, leading to more rapid polysialylation of NCAM without a noticeable increase in the quantities of polySia. Similarly, Beecken et al.[53] demonstrated that valproic acid decreased ST8Sia-II mRNA levels in neuroectodermal tumor cell lines, and they also observed that ST8Sia-IV mRNA levels increased in a compensatory fashion leading to a decrease in the extent of tumor cell adhesion. Ammonia was shown to decrease the level of polySia expression in SCLC cells by altering nucleotide sugar pools; however, this treatment would also be expected to impact general sialylation and perhaps other glycosylation reactions.[54,55] Miyazaki et al.[56] demonstrated that CMP and 2′-*O*-methyl-CMP, general inhibitors of sialyltransferases, could inhibit the activities of ST8Sia-II, -III, and -IV and the polysialylation of NCAM. In more recent work, Al-Saraireh et al.[57] showed that CMP blocked NCAM polysialylation by ST8Sia-II and tumor cell migration. It is important to point out that CMP and its analogues are likely to be nonspecific inhibitors in that they would expected to inhibit other sialyltransferases. As an alternative, we suggest that the limited substrate specificity of the polySTs makes the polyST–substrate interaction interface an attractive drug target. Shiga toxin B subunit-based approaches and pH sensitive liposomes have been useful for the targeted delivery of therapeutics to the secretory pathway.[58–61] Using similar delivery mechanisms, one could envision that therapeutic reagents based on the polyST PBR peptide could be used to block the polyST–substrate interactions in the Golgi and subsequent polysialylation of substrates.

Supplementary Material

Refer to Web version on PubMed Central for supplementary material.

Acknowledgments

Funding

This work was funded by National Institutes of Health Grant RO1 GM101949 (to K.J.C.).

The authors thank Dr. Joseph Zapater for the 6xHis-SUM-OPBR construct and Dr. Matthew Thompson for allowing us report his unpublished work.

ABBREVIATIONS

polySia	polysialic acid
NCAM	neural cell adhesion molecule
FN1	first fibronectin type III repeat of NCAM
Ig5	fifth immunoglobulin domain of NCAM
polyST	polysialyltransferase
PBR	polybasic region
ITC	isothermal titration calorimetry
NMR	nuclear magnetic resonance
NRP-2	neuropilin-2
SCLC	small cell lung carcinoma
DMEM	Dulbecco's modified Eagle's medium
IPTG	isopropyl β-D-1-thiogalactopyranoside
MES	2-(*N*-morpholino)ethanesulfonic acid
Ni-NTA	nickel-nitrilotriacetic acid
HRP	horseradish peroxidase
FITC	fluorescein isothiocyanate
DAPI	4′,6-diamidino-2-phenylindol
OCAM	olfactory cell adhesion molecule
PSTD	polysialyltransferase domain

References

1. Schnaar RL, Gerardy-Schahn R, Hildebrandt H. Sialic acids in the brain: gangliosides and polysialic acid in nervous system development, stability, disease, and regeneration. Physiol Rev. 2014; 94:461–518. [PubMed: 24692354]
2. Sato C, Kitajima K. Disialic, oligosialic and polysialic acids: distribution, functions and related disease. J Biochem. 2013; 154:115–136. [PubMed: 23788662]
3. Colley KJ, Kitajima K, Sato C. Polysialic acid: Biosynthesis, novel functions and applications. Crit Rev Biochem Mol Biol. 2014; 49:498–532. [PubMed: 25373518]

4. Zuber C, Lackie PM, Catterall WA, Roth J. Polysialic acid is associated with sodium channels and the neural cell adhesion molecule N-CAM in adult rat brain. J Biol Chem. 1992; 267:9965–9971. [PubMed: 1315775]
5. Yabe U, Sato C, Matsuda T, Kitajima K. Polysialic acid in human milk. CD36 is a new member of mammalian polysialic acid-containing glycoprotein. J Biol Chem. 2003; 278:13875–13880. [PubMed: 12576469]
6. Werneburg S, Buettner FF, Erben L, Mathews M, Neumann H, Mühlenhoff M, Hildebrandt H. Polysialylation and lipopolysaccharide-induced shedding of E-selectin ligand-1 and neuropilin-2 by microglia and THP-1 macrophages. Glia. 2016; 64:1314–1330. [PubMed: 27159043]
7. Mühlenhoff M, Eckhardt M, Bethe A, Frosch M, Gerardy-Schahn R. Autocatalytic polysialylation of polysialyltransferase-1. EMBO J. 1996; 15:6943–6950. [PubMed: 9003770]
8. Kiermaier E, Moussion C, Veldkamp CT, Gerardy-Schahn R, de Vries I, Williams LG, Chaffee GR, Phillips AJ, Freiberger F, Imre R, Taleski D, Payne RJ, Braun A, Förster R, Mechtler K, Mühlenhoff M, Volkman BF, Sixt M. Polysialylation controls dendritic cell trafficking by regulating chemokine recognition. Science. 2016; 351:186–190. [PubMed: 26657283]
9. James WM, Agnew WS. Multiple oligosaccharide chains in the voltage-sensitive Na channel from electrophorus electricus: evidence for alpha-2,8-linked polysialic acid. Biochem Biophys Res Commun. 1987; 148:817–826. [PubMed: 2446601]
10. Galuska SP, Rollenhagen M, Kaup M, Eggers K, Oltmann-Norden I, Schiff M, Hartmann M, Weinhold B, Hildebrandt H, Geyer R, Mühlenhoff M, Geyer H. Synaptic cell adhesion molecule SynCAM 1 is a target for polysialylation in postnatal mouse brain. Proc Natl Acad Sci U S A. 2010; 107:10250–10255. [PubMed: 20479255]
11. Finne J. Occurrence of unique polysialosyl carbohydrate units in glycoproteins of developing brain. J Biol Chem. 1982; 257:11966–11970. [PubMed: 7118922]
12. Curreli S, Arany Z, Gerardy-Schahn R, Mann D, Stamatos NM. Polysialylated neuropilin-2 is expressed on the surface of human dendritic cells and modulates dendritic cell-T lymphocyte interactions. J Biol Chem. 2007; 282:30346–30356. [PubMed: 17699524]
13. Close BE, Colley KJ. In vivo autopolysialylation and localization of the polysialyltransferases PST and STX. J Biol Chem. 1998; 273:34586–34593. [PubMed: 9852130]
14. Rutishauser U. Polysialic acid in the plasticity of the developing and adult vertebrate nervous system. Nat Rev Neurosci. 2008; 9:26–35. [PubMed: 18059411]
15. Johnson CP, Fujimoto I, Rutishauser U, Leckband DE. Direct evidence that neural cell adhesion molecule (NCAM) polysialylation increases intermembrane repulsion and abrogates adhesion. J Biol Chem. 2005; 280:137–145. [PubMed: 15504723]
16. Seidenfaden R, Krauter A, Schertzinger F, Gerardy-Schahn R, Hildebrandt H. Polysialic acid directs tumor cell growth by controlling heterophilic neural cell adhesion molecule interactions. Mol Cell Biol. 2003; 23:5908–5918. [PubMed: 12897159]
17. Eggers K, Werneburg S, Schertzinger A, Abeln M, Schiff M, Scharenberg MA, Burkhardt H, Mühlenhoff M, Hildebrandt H. Polysialic acid controls NCAM signals at cell-cell contacts to regulate focal adhesion independent from FGF receptor activity. J Cell Sci. 2011; 124:3279–3291. [PubMed: 21940794]
18. Weinhold B, Seidenfaden R, Rockle I, Mühlenhoff M, Schertzinger F, Conzelmann S, Marth JD, Gerardy-Schahn R, Hildebrandt H. Genetic ablation of polysialic acid causes severe neurodevelopmental defects rescued by deletion of the neural cell adhesion molecule. J Biol Chem. 2005; 280:42971–42977. [PubMed: 16267048]
19. Tsuchiya A, Lu WY, Weinhold B, Boulter L, Stutchfield BM, Williams MJ, Guest RV, Minnis-Lyons SE, Mackinnon AC, Schwarzer D, Ichida T, Nomoto M, Aoyagi Y, Gerardy-Schahn R, Forbes SJ. PolySia-NCAM modulates the formation of ductular reactions in liver injury. Hepatology. 2014; 60:1727–1740. [PubMed: 24585441]
20. El Maarouf A, Petridis AK, Rutishauser U. Use of polysialic acid in repair of the central nervous system. Proc Natl Acad Sci U S A. 2006; 103:16989–16994. [PubMed: 17075041]
21. Wang X, Li X, Zeng YN, He F, Yang XM, Guan F. Enhanced expression of polysialic acid correlates with malignant phenotype in breast cancer cell lines and clinical tissue samples. Int J Mol Med. 2016; 37:197–206. [PubMed: 26530860]

22. Falconer RA, Errington RJ, Shnyder SD, Smith PJ, Patterson LH. Polysialyltransferase: a new target in metastatic cancer. Curr Cancer Drug Targets. 2012; 12:925–939. [PubMed: 22463390]
23. Nelson RW, Bates PA, Rutishauser U. Protein determinants for specific polysialylation of the neural cell adhesion molecule. J Biol Chem. 1995; 270:17171–17179. [PubMed: 7615513]
24. Thompson MG, Foley DA, Swartzentruber KG, Colley KJ. Sequences at the interface of the fifth immunoglobulin domain and first fibronectin type III repeat of the neural cell adhesion molecule are critical for its polysialylation. J Biol Chem. 2011; 286:4525–4534. [PubMed: 21131353]
25. Mendiratta SS, Sekulic N, Lavie A, Colley KJ. Specific amino acids in the first fibronectin type III repeat of the neural cell adhesion molecule play a role in its recognition and polysialylation by the polysialyltransferase ST8Sia IV/PST. J Biol Chem. 2005; 280:32340–32348. [PubMed: 16027151]
26. Close BE, Mendiratta SS, Geiger KM, Broom LJ, Ho LL, Colley KJ. The minimal structural domains required for neural cell adhesion molecule polysialylation by PST/ST8Sia-IV and STX/ST8Sia-II. J Biol Chem. 2003; 278:30796–30805. [PubMed: 12791681]
27. Mendiratta SS, Sekulic N, Hernandez-Guzman FG, Close BE, Lavie A, Colley KJ. A novel alpha-helix in the first fibronectin type III repeat of the neural cell adhesion molecule is critical for N-glycan polysialylation. J Biol Chem. 2006; 281:36052–36059. [PubMed: 17003032]
28. Foley DA, Swartzentruber KG, Lavie A, Colley KJ. Structure and mutagenesis of neural cell adhesion molecule domains: evidence for flexibility in the placement of polysialic acid attachment sites. J Biol Chem. 2010; 285:27360–27371. [PubMed: 20573953]
29. Thompson MG, Foley DA, Colley KJ. The polysialyltransferases interact with sequences in two domains of the neural cell adhesion molecule to allow its polysialylation. J Biol Chem. 2013; 288:7282–7293. [PubMed: 23341449]
30. Bhide GP, Fernandes NR, Colley KJ. Sequence requirements for neuropilin-2 recognition by ST8SiaIV and polysialylation of Its O-glycans. J Biol Chem. 2016; 291:9444–9457. [PubMed: 26884342]
31. Rollenhagen M, Kuckuck S, Ulm C, Hartmann M, Galuska SP, Geyer R, Geyer H, Mühlenhoff M. Polysialylation of the synaptic cell adhesion molecule 1 (SynCAM 1) depends exclusively on the polysialyltransferase ST8SiaII in vivo. J Biol Chem. 2012; 287:35170–35180. [PubMed: 22908220]
32. Datta AK, Paulson JC. Sialylmotifs of sialyltransferases. Indian J Biochem Biophys. 1997; 34:157–165. [PubMed: 9343944]
33. Audry M, Jeanneau C, Imberty A, Harduin-Lepers A, Delannoy P, Breton C. Current trends in the structure-activity relationships of sialyltransferases. Glycobiology. 2011; 21:716–726. [PubMed: 21098518]
34. Zapater JL, Colley KJ. Sequences prior to conserved catalytic motifs of polysialyltransferase ST8Sia IV are required for substrate recognition. J Biol Chem. 2012; 287:6441–6453. [PubMed: 22184126]
35. Nakata D, Zhang L, Troy FA 2nd. Molecular basis for polysialylation: a novel polybasic polysialyltransferase domain (PSTD) of 32 amino acids unique to the alpha 2,8-polysialyltransferases is essential for polysialylation. Glycoconjugate J. 2006; 23:423–436.
36. Foley DA, Swartzentruber KG, Colley KJ. Identification of sequences in the polysialyltransferases ST8Sia II and ST8Sia IV that are required for the protein-specific polysialylation of the neural cell adhesion molecule, NCAM. J Biol Chem. 2009; 284:15505–15516. [PubMed: 19336400]
37. Meng L, Forouhar F, Thieker D, Gao Z, Ramiah A, Moniz H, Xiang Y, Seetharaman J, Milaninia S, Su M, Bridger R, Veillon L, Azadi P, Kornhaber G, Wells L, Montelione GT, Woods RJ, Tong L, Moremen KW. Enzymatic basis for N-glycan sialylation: structure of rat alpha2,6-sialyltransferase (ST6GAL1) reveals conserved and unique features for glycan sialylation. J Biol Chem. 2013; 288:34680–34698. [PubMed: 24155237]
38. Volkers G, Worrall LJ, Kwan DH, Yu CC, Baumann L, Lameignere E, Wasney GA, Scott NE, Wakarchuk W, Foster LJ, Withers SG, Strynadka NC. Structure of human ST8SiaIII sialyltransferase provides insight into cell-surface polysialylation. Nat Struct Mol Biol. 2015; 22:627–635. [PubMed: 26192331]

39. Rao FV, Rich JR, Rakic B, Buddai S, Schwartz MF, Johnson K, Bowe C, Wakarchuk WW, Defrees S, Withers SG, Strynadka NC. Structural insight into mammalian sialyltransferases. Nat Struct Mol Biol. 2009; 16:1186–1188. [PubMed: 19820709]
40. Kuhn B, Benz J, Greif M, Engel AM, Sobek H, Rudolph MG. The structure of human alpha-2,6-sialyltransferase reveals the binding mode of complex glycans. Acta Crystallogr, Sect D: Biol Crystallogr. 2013; 69:1826–1838. [PubMed: 23999306]
41. Shen Y, Delaglio F, Cornilescu G, Bax A. TALOS+: a hybrid method for predicting protein backbone torsion angles from NMR chemical shifts. J Biomol NMR. 2009; 44:213–223. [PubMed: 19548092]
42. Delaglio F, Grzesiek S, Vuister GW, Zhu G, Pfeifer J, Bax A. NMRPipe: a multidimensional spectral processing system based on UNIX pipes. J Biomol NMR. 1995; 6:277–293. [PubMed: 8520220]
43. Zhou GP, Huang RB, Troy FA II. 3D structural conformation and functional domains of polysialyltransferase ST8Sia IV required for polysialylation of neural cell adhesion molecules. Protein Pept Lett. 2015; 22:137–148. [PubMed: 25329332]
44. Sturtevant JM. Heat capacity and entropy changes in processes involving proteins. Proc Natl Acad Sci U S A. 1977; 74:2236–2240. [PubMed: 196283]
45. MacRaild CA, Daranas AH, Bronowska A, Homans SW. Global changes in local protein dynamics reduce the entropic cost of carbohydrate binding in the arabinose-binding protein. J Mol Biol. 2007; 368:822–832. [PubMed: 17368482]
46. Sattler M, Schleucher J, Griesinger C. Heteronuclear multidimensional NMR experiments for the structure determination of proteins in solution employing pulsed field gradients. Prog Nucl Magn Reson Spectrosc. 1999; 34:93–158.
47. Baker NA, Sept D, Joseph S, Holst MJ, McCammon JA. Electrostatics of nanosystems: application to microtubules and the ribosome. Proc Natl Acad Sci U S A. 2001; 98:10037–10041. [PubMed: 11517324]
48. Foley DA, Swartzentruber KG, Thompson MG, Mendiratta SS, Colley KJ. Sequences from the first fibronectin type III repeat of the neural cell adhesion molecule allow O-glycan polysialylation of an adhesion molecule chimera. J Biol Chem. 2010; 285:35056–35067. [PubMed: 20805222]
49. Kulahin N, Kristensen O, Rasmussen KK, Olsen L, Rydberg P, Vestergaard B, Kastrup JS, Berezin V, Bock E, Walmod PS, Gajhede M. Structural model and transinteraction of the entire ectodomain of the olfactory cell adhesion molecule. Structure. 2011; 19:203–211. [PubMed: 21300289]
50. Rillahan CD, Antonopoulos A, Lefort CT, Sonon R, Azadi P, Ley K, Dell A, Haslam SM, Paulson JC. Global metabolic inhibitors of sialyl- and fucosyltransferases remodel the glycome. Nat Chem Biol. 2012; 8:661–668. [PubMed: 22683610]
51. Macauley MS, Arlian BM, Rillahan CD, Pang PC, Bortell N, Marcondes MC, Haslam SM, Dell A, Paulson JC. Systemic blockade of sialylation in mice with a global inhibitor of sialyltransferases. J Biol Chem. 2014; 289:35149–35158. [PubMed: 25368325]
52. Seidenfaden R, Hildebrandt H. Retinoic acid-induced changes in polysialyltransferase mRNA expression and NCAM polysialylation in human neuroblastoma cells. J Neurobiol. 2001; 46:11–28. [PubMed: 11108612]
53. Beecken WD, Engl T, Ogbomo H, Relja B, Cinatl J, Bereiter-Hahn J, Oppermann E, Jonas D, Blaheta RA. Valproic acid modulates NCAM polysialylation and polysialyltransferase mRNA expression in human tumor cells. Int Immunopharmacol. 2005; 5:757–769. [PubMed: 15710344]
54. Zanghi JA, Mendoza TP, Schmelzer AE, Knop RH, Miller WM. Role of nucleotide sugar pools in the inhibition of NCAM polysialylation by ammonia. Biotechnol Prog. 1998; 14:834–844. [PubMed: 9841644]
55. Zanghi JA, Mendoza TP, Knop RH, Miller WM. Ammonia inhibits neural cell adhesion molecule polysialylation in Chinese hamster ovary and small cell lung cancer cells. J Cell Physiol. 1998; 177:248–263. [PubMed: 9766522]
56. Miyazaki T, Angata K, Seeberger PH, Hindsgaul O, Fukuda M. CMP substitutions preferentially inhibit polysialic acid synthesis. Glycobiology. 2008; 18:187–194. [PubMed: 18077550]
57. Al-Saraireh YM, Sutherland M, Springett BR, Freiberger F, Ribeiro Morais G, Loadman PM, Errington RJ, Smith PJ, Fukuda M, Gerardy-Schahn R, Patterson LH, Shnyder SD, Falconer RA.

Pharmacological inhibition of polysialyltransferase ST8SiaII modulates tumour cell migration. PLoS One. 2013; 8:e73366. [PubMed: 23951351]

58. Sandvig K, van Deurs B. Delivery into cells: lessons learned from plant and bacterial toxins. Gene Ther. 2005; 12:865–872. [PubMed: 15815697]
59. Johannes L, Romer W. Shiga toxins–from cell biology to biomedical applications. Nat Rev Microbiol. 2010; 8:105–116. [PubMed: 20023663]
60. Haicheur N, Bismuth E, Bosset S, Adotevi O, Warnier G, Lacabanne V, Regnault A, Desaymard C, Amigorena S, Ricciardi-Castagnoli P, Goud B, Fridman WH, Johannes L, Tartour E. The B subunit of Shiga toxin fused to a tumor antigen elicits CTL and targets dendritic cells to allow MHC class I-restricted presentation of peptides derived from exogenous antigens. J Immunol. 2000; 165:3301–3308. [PubMed: 10975847]
61. Costin GE, Trif M, Nichita N, Dwek RA, Petrescu SM. pH-sensitive liposomes are efficient carriers for endoplasmic reticulum-targeted drugs in mouse melanoma cells. Biochem Biophys Res Commun. 2002; 293:918–923. [PubMed: 12051746]
62. Robert X, Gouet P. Deciphering key features in protein structures with the new ENDscript server. Nucleic Acids Res. 2014; 42:W320–324. [PubMed: 24753421]

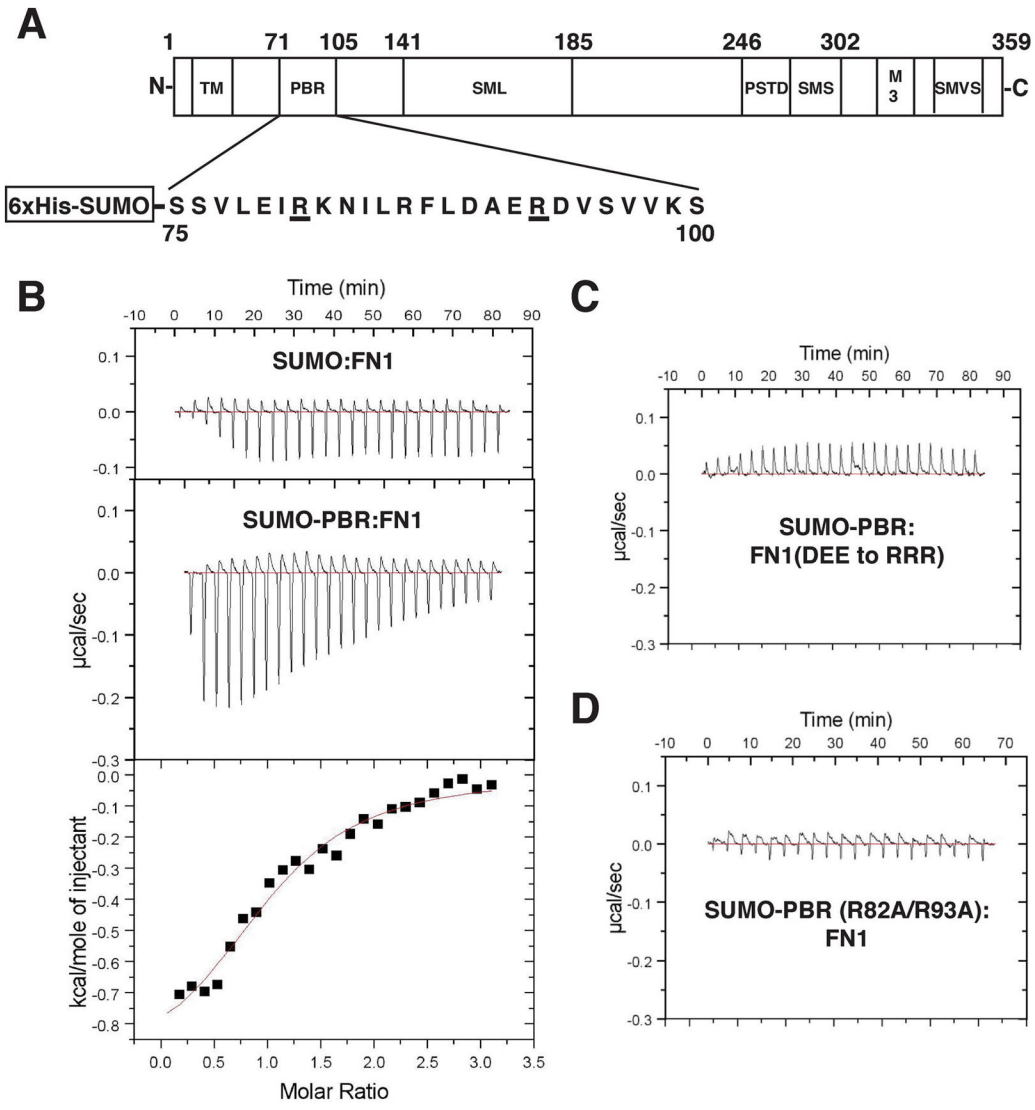

Figure 1.

Isothermal titration calorimetry of SUMO-PBR and NCAM FN1. (A) Schematic of the domain structure and conserved sequences in ST8Sia-IV. Shown are sialyl motifs that are conserved in all sialyltransferases [large (SML), small (SMS), motif 3 (M3), and very small (SMVS)], as well as two regions unique to polySTs, the polybasic region (PBR) and the polysialyltransferase domain (PSTD). The sequence of the PBR peptide used in in this study is shown with R82 and R83, key residues for NCAM recognition and polysialylation, underlined. (B) Heat exchanges resulting from a control titration between FN1 and SUMO (top panel). Heat exchanges and calculated enthalpies resulting from the titration of 600 μM SUMO-PBR with 20 μM FN1 (bottom panels). (C) The FN1 ^{520}DEE^{523} to RRR mutation that leads to an elimination of NCAM polysialylation[25] also leads to a loss of binding between SUMO-PBR and FN1. (D) The ST8Sia-IV PBR R82A/R93A mutation that leads to a loss of NCAM polysialylation also leads to a loss of binding between the PBR and FN1 domain.

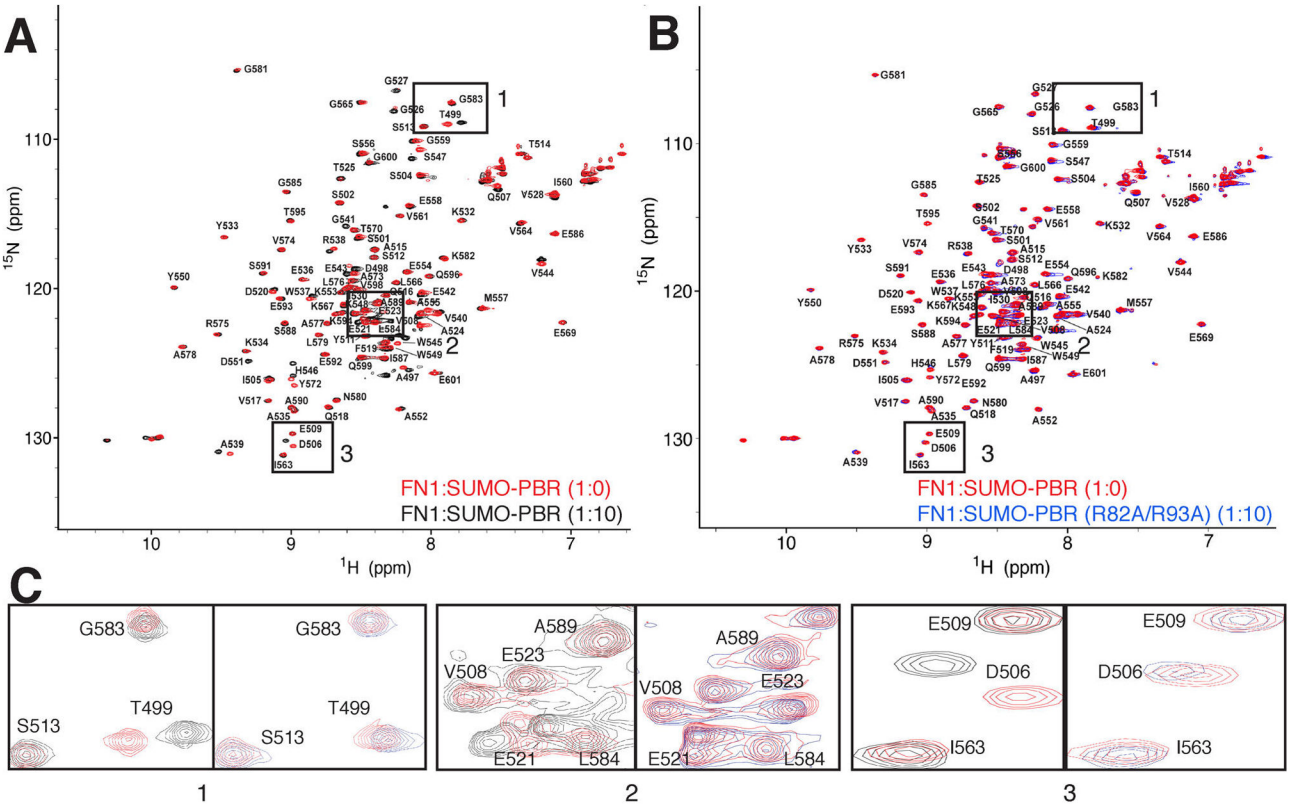

Figure 2.

^{1}H–^{15}N HSQC NMR spectra for ^{15}N-labeled NCAM FN1 with and without titration with the SUMO-PBR peptides. (A) Overlay of the ^{1}H–^{15}N HSQC NMR spectrum of the ^{15}N-labeled FN1 domain (red) and the spectrum after addition of the unlabeled SUMO-PBR peptide at a 1:10 concentration ratio (black). (B) As a control, the ^{15}N-labeled FN1 domain spectrum (red) was overlaid with that obtained after addition of the nonbinding SUMO-PBR (R82A/R93A) mutant (blue) at a 1:10 concentration ratio. Other titrations have been omitted for the sake of clarity. (C) Selected interacting residues [Thr^{499} (box 1), Glu^{521} (box 2), and Asp^{506} (box 3)] showing specific chemical exchanges for wild-type SUMO-PBR but not SUMO-PBR (R82A/R93A) are magnified with spectra from panel A on the left and panel B on the right.

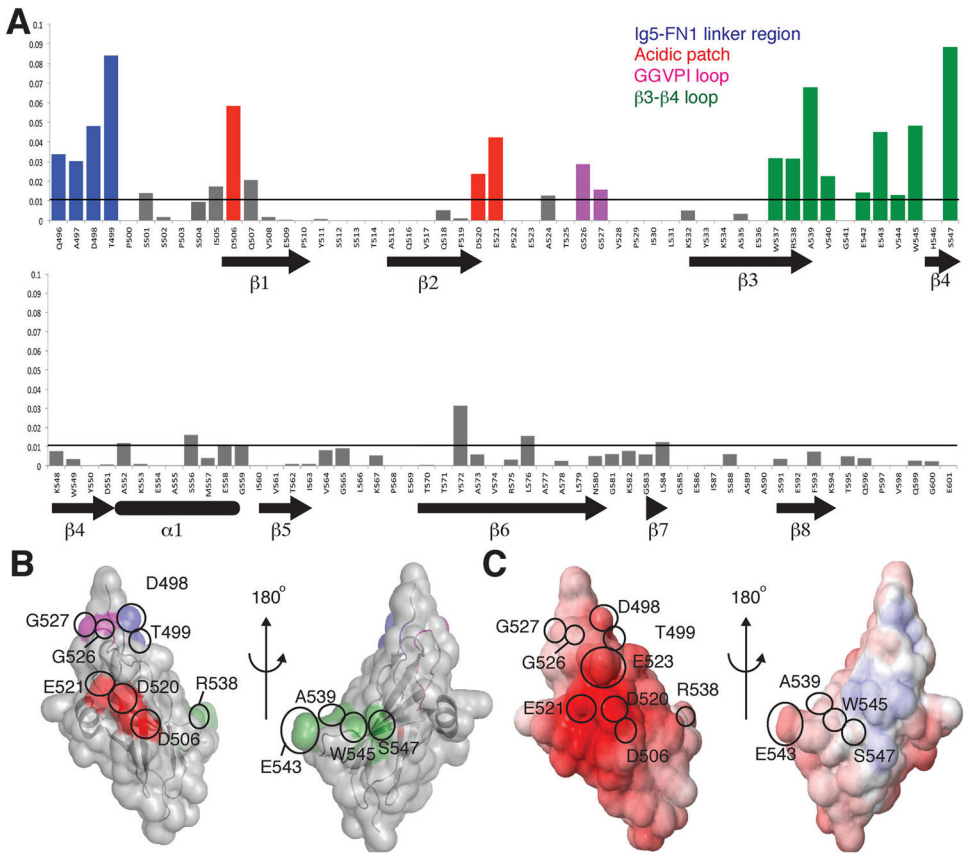

Figure 3.

NCAM FN1 residues impacted by ST8Sia-IV PBR peptide binding. (A) Residues showing specific and significant NMR chemical shift perturbations upon addition of the SUMO-PBR peptide. The combined shift difference (CSD) values for the FN1–SUMO-PBR interaction were plotted after subtraction of the control values, and the data are presented as two bar graphs representing the N-terminal (top) and C-terminal (bottom) residues of the FN1 domain. (B) The FN1 residues most impacted by SUMO-PBR interaction are mapped onto the crystal structure of the FN1 domain (PDB entry 2HAZ).[27] (C) Electrostatic surface potential map of NCAM FN1 calculated using the Adaptive Poisson–Boltzmann Solver (APBS).[47] For both panels B and C, two views of the NCAM FN1 domain structure are shown rotated by 180°.

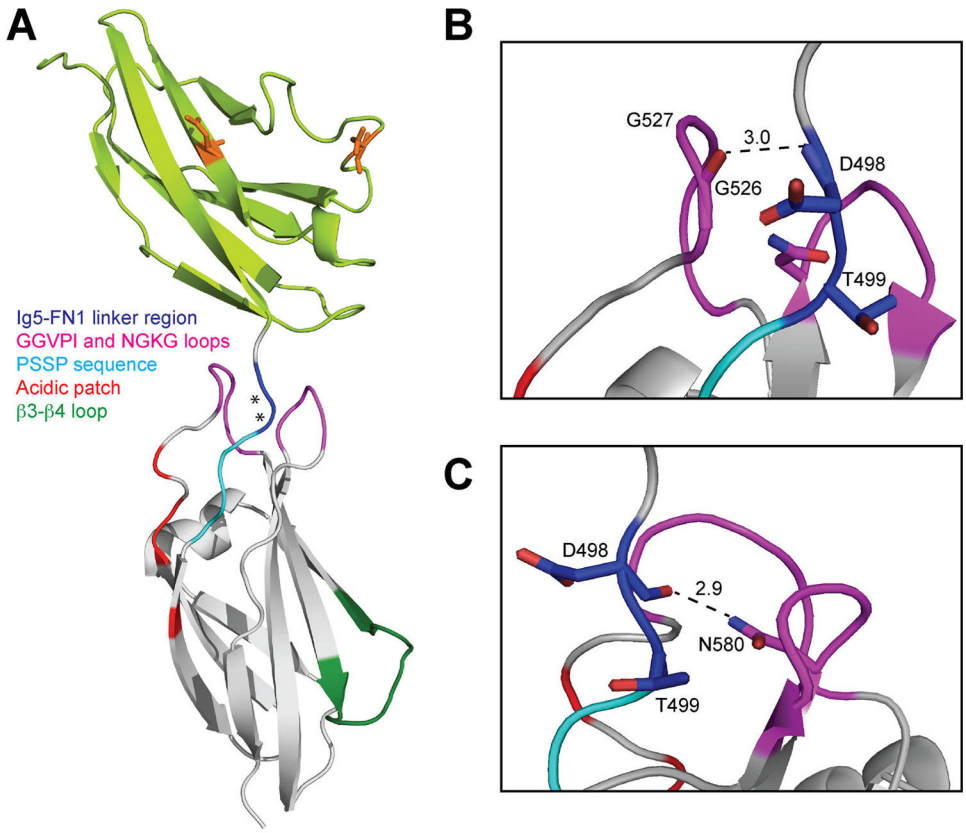

Figure 4.

NCAM Ig5–FN1 structure and interactions between the linker region and FN1 GGVPI and NGKG loops. (A) Crystal structure of the NCAM Ig5–FN1 linker region (PDB entry 3MTR).[28] Asparagine residues in the Ig5 domain bearing *N*-glycans that are polysialylated are colored orange. The Ig5–FN1 linker region, including Gln^{496}, Ala^{497}, Asp^{498}, and Thr^{499}, is colored dark blue with asterisks indicating the positions of Asp^{498} and Thr^{499}. The PSSP sequence, colored cyan, is a part of the same unstructured segment that comprises the linker region. The GGVPI and NGKG loops flanking and stabilizing the linker region are colored magenta. The acidic patch that includes Asp^{506}, Asp^{520}, Glu^{521}, and Glu^{523} is colored red. The $\beta 3$–$\beta 4$ loop that connects strands leading to a unique FN1 α-helix and the GGVPI loop and acidic patch is colored green. (B) Predicted hydrogen bond formed between the main chain amide group of Asp^{498} in the linker region and the main chain carbonyl of Gly^{526} in the GGVPI loop. (C) Predicted hydrogen bond formed between the side chain amide group of Asn^{580} in the NGKG loop and the main chain carbonyl of Asp^{498} in the linker region. This figure is adapted from ref 24.

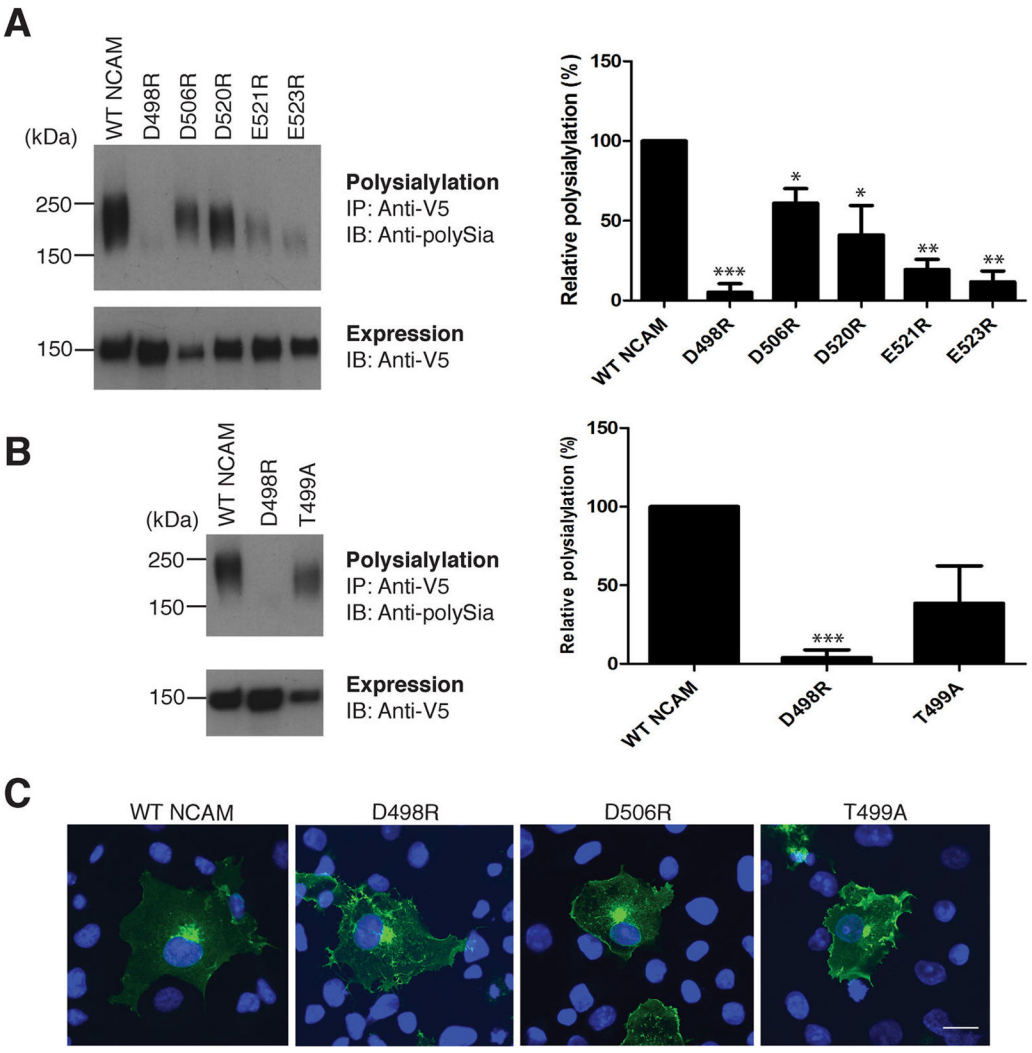

Figure 5.

Impact of acidic patch and linker mutations on NCAM polysialylation. (A) Polysialylation (top) and expression (bottom) of NCAM mutants with replacements of known and potential acidic patch residues. The adjacent bar graph shows statistics resulting from three different experiments. (B) Polysialylation (top) and expression (bottom) of NCAM mutants with replacements of two Ig5–-FN1 linker residues. The adjacent bar graphs show statistics from three different experiments. Quantification of the experimental results in panels A and B was performed as described in Materials and Methods with error bars representing the standard deviation (SD). Statistical analysis was performed using unpaired Student's *t* tests: *$0.01 < p < 0.05$, **$0.001 < p < 0.01$, and ***$0.0001 < p < 0.001$ with respect to wild-type NCAM, which is normalized to 100%. The *p* value for T499A is 0.06. (C) Cellular localization of V5-tagged NCAM mutants in COS-7 cells. V5-tagged NCAM mutants were localized by indirect immunofluorescence microscopy using a mouse anti-V5 antibody and a FITC-conjugated goat anti-mouse antibody. DAPI is used to stain the cell nucleus. The scale bar is 20 μm.

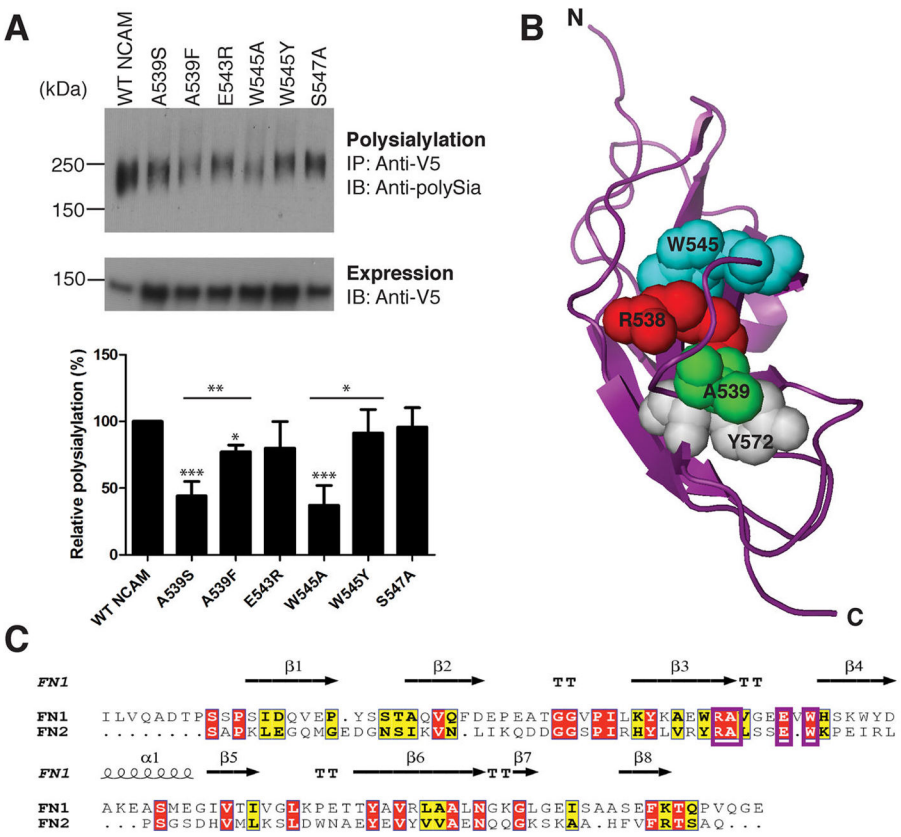

Figure 6.

Impact of mutating residues in the FN1 β3–β4 loop on NCAM polysialylation. (A) Polysialylation (top) and expression (bottom) of NCAM mutants with replacements of β3–β4 loop residues. The adjacent bar graph shows statistics resulting from three different experiments. Quantification of the experimental results was performed as described in Materials and Methods with error bars representing the SD. Statistical analysis was performed using unpaired Student's *t* tests: *$0.01 < p < 0.05$, **$0.001 < p < 0.01$, and ***$0.0001 < p < 0.001$ with respect to wild-type NCAM, which is normalized to 100%. Other comparisons are indicated by a line above the bars in the graph. (B) Packing of residues in the β3–β4 loop of NCAM FN1. (C) Conservation of the primary sequence between the NCAM FN1 and FN2 domains generated using ESPript.[62] Conserved residues in the β3–β4 loop are boxed. Conserved residues are colored red and similar residues yellow, and purple boxes indicate the β3–β4 loop residues conserved between the NCAM FN1 and NCAM FN2 domains.